ChemPubSoc Europe

DOI: 10.1002/chem.201303925

CHEMISTRY
A European Journal
Full Paper

Metallocenes

Indium-Bridged [1]Ferrocenophanes

Bidraha Bagh,[a, c] Saeid Sadeh,[a] Jennifer C. Green,[b] and Jens Müller*[a]

Abstract: Indium-bridged [1]ferrocenophanes ([1]FCPs) and [1.1]ferrocenophanes ([1.1]FCPs) were synthesized from dilithioferrocene species and indium dichlorides. The reaction of Li_2fc·tmeda (fc = $(H_4C_5)_2Fe$) and (Mamx)$InCl_2$ (Mamx = 6-(Me_2NCH_2)-2,4-*t*$Bu_2C_6H_2$) gave a mixture of the [1]FCP (Mamx)Infc (**4**$_1$), the [1.1]FCP [(Mamx)Infc]$_2$ (**4**$_2$), and oligomers [(Mamx)Infc]$_n$ (**4**$_n$). In a similar reaction, employing the enantiomerically pure, planar-chiral (S_p,S_p)-1,1′-dibromo-2,2′-diisopropylferrocene (**1**) as a precursor for the dilithioferrocene derivative Li_2fc^{iPr2}, equipped with two *i*Pr groups in the α position, gave the inda[1]ferrocenophane **5**$_1$ [(Mamx)Infc^{iPr2}] selectively. Species **5**$_1$ underwent ring-opening polymerization to give the polymer **5**$_n$. The reaction between Li_2fc^{iPr2} and Ar′$InCl_2$ (Ar′ = 2-(Me_2NCH_2)C_6H_4) gave an inseparable mixture of the [1]FCP Ar′$Infc^{iPr2}$ (**6**$_1$) and the [1.1]FCP [Ar′$Infc^{iPr2}$]$_2$ (**6**$_2$). Hydrogenolysis reactions (BP86/TZ2P) of the four inda[1]ferrocenophanes revealed that the structurally most distorted species (**5**$_1$) is also the most strained [1]FCP.

Introduction

Over the last two decades, ring-opening polymerization (ROP) of strained ferrocenophanes has been developed into an established method for the preparation of metallopolymers.[1] The most exciting ROPs are living polymerizations, as they allow control of molecular weights and weight distributions. Starting from block copolymers, recent developments in this area led to the preparation of "living" micelles with a poly(ferrocenylsilane) core (ER_x = $SiMe_2$; Figure 1), which upon addition of further unimers gave larger micelles of uniform lengths. This crystallization-driven living self-assembly is a new bottom-up approach to uniform nanomaterials.[2] However, from the large number of [1]ferrocenophanes ([1]FCPs; Figure 1),[3] only those bridged by silicon,[1d,4] germanium,[5] or phosphorus,[6,7] are known to ring-open polymerize in a living fashion. Many others can be polymerized and, presumably, the lack of controlling properties of the resulting polymers through control of molecular weight brought investigations into their chemistry to a standstill.[8] In other cases, the low solubility of resulting polyferrocenes (PFs; Figure 1) in organic solvents prevented their full characterization and processibility for any further uses.[9,10] To take full advantage of the ROP of strained sandwich compounds in the future, either FCPs with different bridging moieties need to be developed or known systems need to be altered so that processible metallopolymers with well-defined molecular weights can be prepared.

In contrast to the large class of silicon-bridged [1]FCPs, knowledge about [1]FCPs containing Group 13 elements in bridging positions is limited. To date, [1]FCPs with boron,[10,11] aluminum,[12] and gallium[11,12b–d,13] in bridging positions are known. In all cases, a combination of steric and electronic stabilization of the Group 13 element had been applied. The known boron-bridged [1]FCPs were equipped with the bulky amino groups $N(SiMe_3)_2$, $N(SiMe_3)$*t*Bu, or N*i*Pr_2,[10] whereas for aluminum and gallium compounds, bulky ligands, capable of intramolecular donation had been employed (Pytsi, Me_2Ntsi, and Mamx; Figure 2). In all cases, the Lewis acidity of the Group 13 element was decreased by electron donation from

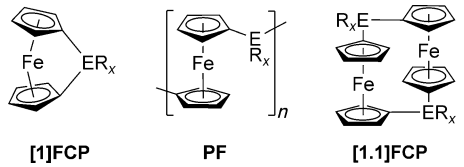

Figure 1. [1]Ferrocenophanes, polyferrocenes, and [1.1]ferrocenophanes.

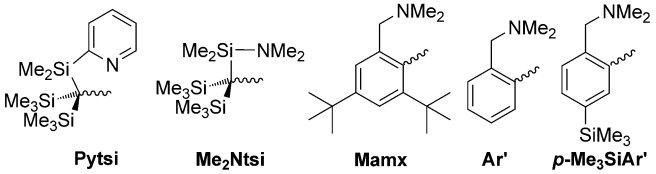

Figure 2. Intramolecularly coordinating ligands.

[a] *Dr. B. Bagh, S. Sadeh, Prof. Dr. J. Müller*
Department of Chemistry, University of Saskatchewan
110 Science Place, Saskatoon, Saskatchewan S7N 5C9 (Canada)
Fax: (+1) 306-966-4730
E-mail: jens.mueller@usask.ca

[b] *Prof. Dr. J. C. Green*
Department of Chemistry, Inorganic Chemistry Laboratory
University of Oxford, Oxford OX1 3QR (UK)

[c] *Dr. B. Bagh*
Present address: Department of Chemistry, University of Toronto
80 St. George Street, Toronto, Ontario M5S 3H6 (Canada)

Supporting information for this article is available on the WWW under http://dx.doi.org/10.1002/chem.201303925.

© 2014 Wiley-VCH Verlag GmbH & Co. KGaA, Weinheim

nitrogen, either through the formation of π (boron) or σ bonds (aluminum and gallium).

Usually, FCPs are synthesized from dilithioferrocene (Li_2fc·tmeda; fc = $(H_4C_5)_2Fe$) and suitable element dihalides R_xEX_2 (the salt-metathesis route), or from pre-linked cyclopentadiene moieties $R_xE(C_5H_5)_2$ through the addition of a base and FeX_2 (the flytrap route).[3a,d,14] The salt-metathesis route is the most common method and had been applied for all Group 13 element-bridged [1]FCPs.[3d] For all these species, the outcome of the salt-metathesis reaction also depends on steric factors. In the case of boron, decreasing the size of the amino group to NMe_2, NMePh, or NMe(*n*Bu) led to the formation of products (presumably polymeric materials) that were insoluble in common organic solvents.[10b,15–17] For aluminum and gallium, employing the non-bulky ligands Ar′ or *p*-Me_3SiAr′ (Figure 2) resulted in the isolation of [1.1]ferrocenophanes[18] ([1.1]FCPs; Figure 1) instead of the targeted [1]FCPs.[19]

Aluminum- or gallium-bridged [1]FCPs equipped with the bulky Pytsi or Me_2Ntsi ligand (Figure 2) were not prone to ROP.[12c] On the other hand, employing the Mamx ligand resulted in [1]FCPs that were surprisingly reactive and polymerized under the conditions of their formation reactions.[13c,d] Recently, we formally moved the bulkiness from the stabilizing ligand onto the ferrocene moiety and prepared species **1** as a new precursor for a dilithioferrocene derivative (Scheme 1).[11] The

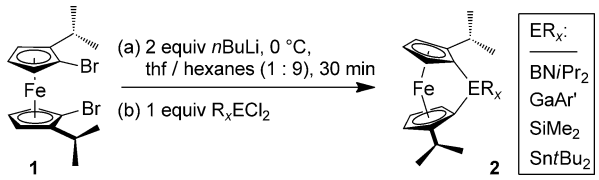

Scheme 1. Synthesis of chiral [1]FCPs.[11]

planar-chiral species **1** was synthesized as an enantiomerically pure compound ((S_p,S_p)-1,1′-dibromo-2,2′-diisopropylferrocene) and gave access to new [1]FCPs (**2**; Scheme 1).[11] Through this tactic, the gallium-bridged species **2**, equipped with the non-bulky Ar′ ligand, was prepared with a high conversion and isolated through crystallization in a yield of 59%. Other species of type **2** are volatile and were purified by sublimation in vacuo, including the highly strained bora[1]ferrocenophane **2** (ER_x = $BNiPr_2$).[11]

Herein, we describe the preparation of the first indium-bridged [1]FCPs, where bulky alkyl groups were used on the ferrocene moiety as well as on the "one-armed" phenyl ligand (Mamx; Figure 2). Spectroscopic data were obtained experimentally, while structural and thermodynamic data were accessed by DFT calculations.

Results and Discussion

Lithiation of (Mamx)Br[11,20] followed by addition of 1 equiv of $InCl_3$ resulted in (Mamx)$InCl_2$ (**3**) (Scheme 2), which was obtained in a moderate yield of 44% and characterized by stan-

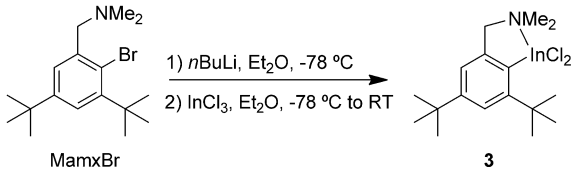

Scheme 2. Synthesis of (Mamx)$InCl_2$ (**3**).

dard methods (^{1}H and ^{13}C NMR spectroscopy, MS, and elemental analysis). ^{1}H and ^{13}C NMR spectra show signal patterns that can be interpreted as being caused by a monomeric species with a time-averaged C_s symmetry. Consistently, mass spectrometry of **3** showed the highest detected mass for the molecular ion of the monomer.[21]

The addition of a solution of **3** in diethyl ether to a suspension of Li_2fc·tmeda in the same solvent gave a mixture of species, as evident from proton NMR spectroscopy (Scheme 3).

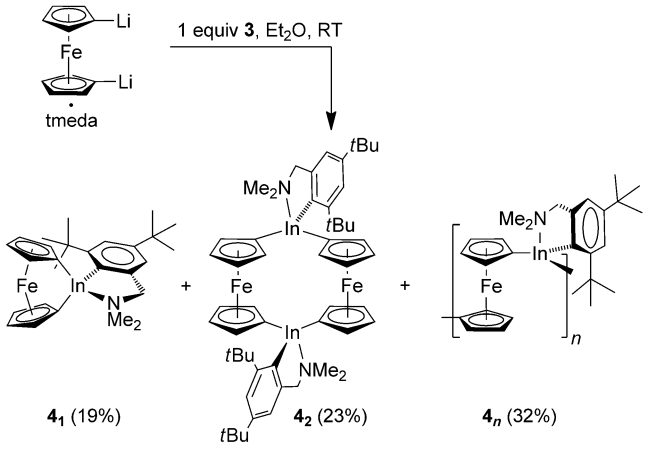

Scheme 3. Reaction of indigane **3** with dilithioferrocene.

After LiCl was removed by filtration, precipitation procedures lead to the isolation of the targeted monomer $\mathbf{4_1}$, the dimer $\mathbf{4_2}$, and the polymeric fraction $\mathbf{4}_n$.

Species $\mathbf{4_1}$ and $\mathbf{4_2}$ were characterized by ^{1}H and ^{13}C NMR spectroscopy, mass spectrometry, and elemental analysis. Mass spectra of both species clearly showed the highest detected masses for M^+, revealing that one species is a [1]FCP ($\mathbf{4_1}$) while the other is a [1.1]FCP ($\mathbf{4_2}$). Species $\mathbf{4_1}$ shows the expected signal pattern in NMR spectra for a C_s symmetric [1]FCP. The most significant resonances are those in the Cp range of the ^{1}H NMR spectrum at $\delta = 4.22$ (2 α-H), 4.39 (2 α-H), 4.41 (2 β-H) and 4.46 ppm (2 β-H). This characteristic signal pattern, with β protons resonating downfield with a small peak separation ($\Delta\delta = 0.05$ ppm) and α protons exhibiting a significantly larger separation ($\Delta\delta = 0.17$ ppm), has been found for all heavier Group 13 element bridged [1]FCPs with C_s symmetry (bridging moiety Ga(Pytsi): $\delta = 4.08$ (2 α-H), 4.45 (2 α-H), 4.61 (2 β-H), and 4.65 ppm (2 β-H);[13a] Ga(Mamx): $\delta = 4.01$ (2 α-H), 4.56 (2 α-H), and 4.69 ppm (4 β-H);[13c] Al(Pytsi): $\delta = 3.91$ (2 α-H), 4.31 (2 α-H), 4.64 (2 β-H), and 4.68 ppm (2 β-H);[12a] Al(Mamx): δ 3.85

© 2014 Wiley-VCH Verlag GmbH & Co. KGaA, Weinheim

(2 α-H), 4.51 (2 α-H), 4.70 (2 β-H), and 4.72 ppm (2 β-H)).[13d] Unfortunately, all attempts at crystallization of $\mathbf{4_1}$ were unsuccessful.

The [1.1]FCP $\mathbf{4_2}$ shows a signal pattern in NMR spectra that could be interpreted as being caused by C_{2h} symmetric species (Scheme 3). For example, the ^{1}H NMR spectrum of $\mathbf{4_2}$ displays three signals in the characteristic range of Cp protons, with one signal being twice as intense as the other two ($\delta = 3.91$ (4 α-H), 4.26 (8 β-H), and 4.40 ppm (4 α-H)). This pattern is a distinctive signature of heavier Group 13 element bridged [1.1]FCPs stabilized by "one-armed" phenyl ligands.[18a,b,d,22] The two signals of the β protons, either with a small splitting or overlapping, appear approximately in the middle of the two signals of the α protons, which, in turn, show a large splitting (In(Me$_2$Ntsi): $\delta = 4.36$ (2 α-H), 4.43 (2 β-H), 4.45 (2 β-H), and 4.57 ppm (2 α-H);[22] InAr′: $\delta = 4.04$ (4 α-H), 4.45 (4 β-H), 4.53 (4 β-H), and 4.97 ppm (4 α-H);[18b] GaAr′: $\delta = 3.99$ (4 α-H), 4.37 (4 β-H), 4.48 (4 β-H), and 5.07 ppm (4 α-H);[18b] AlAr′: $\delta = 3.97$ (4 α-H), 4.42 (4 β-H), 4.52 (4 β-H), and 5.17 ppm (4 α-H)).[18a,23]

Sample $\mathbf{4}_n$ was the third isolated fraction from the salt-metathesis reaction shown in Scheme 3. Broad, multiple peaks in the ^{1}H NMR spectrum of $\mathbf{4}_n$ suggest that this fraction consisted of a mixture of polymers or oligomers. This speculation was confirmed by dynamic light scattering (DLS) analysis, which gave a hydrodynamic radius (R_h) for $\mathbf{4}_n$ of 1.0 ± 0.1 nm. Using the same method as applied for aluminum or gallium-bridged polyferrocenes before,[12d,13c,d] an average molecular weight (M_w) of 4.8 ± 0.8 kDa (about 9 repeating units) was calculated from the measured R_h (for details, see the Experimental Section and the Supporting Information).

As discussed above, we recently prepared the new [1]FCPs of type **2** equipped with two *i*Pr groups in α positions on Cp (Scheme 1). The *i*Pr groups were introduced to prevent the formation of unwanted [1.1]FCPs in salt-metathesis reactions of dilithioferrocene and aluminum or gallium dichlorides. This tactic led to the isolation of the gallium-bridged [1]FCP **2** stabilized with the non-bulky Ar′ ligand (Figure 2). Consequently, the applicability of the same chemistry toward the preparation of inda[1]ferrocenophanes was explored.

As illustrated in Scheme 4, the enantiomerically pure ferrocene dibromide **1** was first lithiated,[11] followed by reaction with (Mamx)InCl$_2$ (**3**) to give the targeted inda[1]ferrocenophane $\mathbf{5_1}$. Reaction control by ^{1}H NMR spectroscopy revealed that the asymmetric species $\mathbf{5_1}$ formed selectively (Supporting Information). For example, in the ^{1}H NMR spectrum four doublets occur for the four methyl groups of the two *i*Pr groups,

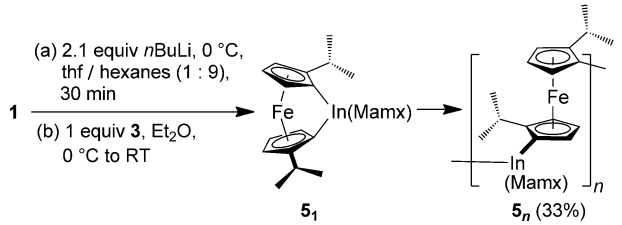

Scheme 4. Synthesis of intermediate $\mathbf{5_1}$ and polymer $\mathbf{5}_n$.

each with an intensity of three relative to each of the six signals in the Cp range ($\delta = 3.68$–4.73 ppm). Furthermore, the Mamx ligand gives rise to two resonances in the aromatic region, two singlets for the *t*Bu groups, two doublets at $\delta =$ 2.65 and 3.94 ppm (CH$_2$), and two singlets at $\delta = 1.91$ and 2.30 ppm (NMe$_2$). The fact that the N-bound methyl groups are non-equivalent is strong evidence for the presence of a nitrogen–indium donor–acceptor bond. Without coordination of the Me$_2$N, only one singlet for both Me groups is expected, as a fast inversion at nitrogen would allow for a fast swapping between the two positions of the methyl groups. The recently characterized [1]FCP **2** (ER$_x$ = GaAr′; Scheme 1) is the most suitable compound for comparison to species $\mathbf{5_1}$. Both species exhibit C_1 symmetry and have the same ferrocenediyl moiety in common. Thus, the pattern of the six Cp protons and their chemical shifts should be similar, which is indeed the case ($\mathbf{5_1}$: $\delta = 3.68$, 4.11 (α-H), 4.47, 4.50, 4.67, 4.73 ppm (β-H); **2** (ER$_x$ = GaAr′): $\delta = 3.53$, 3.98 (α-H), 4.46, 4.50, 4.67, 4.70 ppm (β-H)). As discussed above for species $\mathbf{4_1}$, the peak separation for α and β protons are significantly different and $\mathbf{5_1}$ and **2** (ER$_x$ = GaAr′) are no exception; the peak separations of the α protons are significantly larger ($\mathbf{5_1}$: $\Delta\delta = 0.43$ ppm; **2** (ER$_x$ = GaAr′): $\Delta\delta =$ 0.45 ppm) than those of β protons ($\mathbf{5_1}$: $\Delta\delta = 0.26$ ppm; **2** (ER$_x$ = GaAr′): $\Delta\delta = 0.24$ ppm).

Unfortunately, all attempts to isolate $\mathbf{5_1}$ failed as this strained monomer polymerized in the reaction mixture resulting in the poly(ferrocenylindigane) $\mathbf{5}_n$ (see the Experimental Section). The ^{1}H NMR spectrum shows broad peaks in the expected areas for the different types of protons. DLS analysis of the sample dissolved in thf gave an R_h of 2.4 ± 0.1 nm, resulting in a calculated $M_w = 24 \pm 2$ kDa (about 38 repeating units with respect to poly(ferrocenyldimethylsilane) (PFS)[24] (see the Experimental Section and Supporting Information).

The chemical behaviour of the indium species $\mathbf{5_1}$ is reminiscent of the strained sandwich compounds (Mamx)Gafc and (Mamx)Alfc.[13c,18d] Both [1]FCPs as well as their ruthenium analogues spontaneously polymerize in solution.[13c,18d] However, to perform controlled polymerizations, monomers must be isolated and purified. Against the background that the use of two *i*Pr groups on the ferrocenediyl moiety resulted in the isolation of the gallane **2** (ER$_x$ = GaAr′; Scheme 1),[11] the salt metathesis of the dilithio derivative of **1** and Ar′InCl$_2$ was performed with the hope that predominantly the targeted inda[1]ferrocenophane $\mathbf{6_1}$ forms (Scheme 5). However, a mixture of the targeted [1]FCP $\mathbf{6_1}$ and the [1.1]FCP $\mathbf{6_2}$ was obtained from the salt-metathesis reaction (Scheme 5). Unfortunately, using a similar workup procedure as for species of type **4**, the new compounds $\mathbf{6_1}$ and $\mathbf{6_2}$ could not be separated. Estimated from a ^{1}H NMR spectrum taken from an aliquot of the reaction mixture about 10 min after the addition of Ar′InCl$_2$, the [1.1]FCP $\mathbf{6_2}$ is the major product with both species being formed in an approximate molar ratio of 1.0:0.86. Even though we could not isolate one of the products, both species could unequivocally be identified by ^{1}H NMR spectroscopy. Species $\mathbf{6_1}$ (C_1 symmetry) and $\mathbf{6_2}$ (C_2 symmetry) are expected to show the same number of signals. The distinctively different peak pattern caused by the Cp clearly reveals that a [1]FCP and a [1.1]FCP

© 2014 Wiley-VCH Verlag GmbH & Co. KGaA, Weinheim

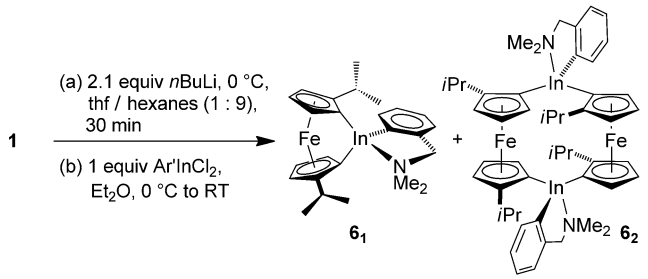

Scheme 5. Inseparable product mixture of $\mathbf{6_1}$ and $\mathbf{6_2}$ identified by ^{1}H NMR spectroscopy.

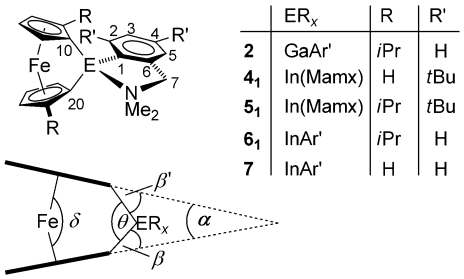

	ER_x	R	R'
2	GaAr'	*i*Pr	H
$\mathbf{4_1}$	In(Mamx)	H	*t*Bu
$\mathbf{5_1}$	In(Mamx)	*i*Pr	*t*Bu
$\mathbf{6_1}$	InAr'	*i*Pr	H
7	InAr'	H	H

Figure 3. Calculated molecules and the set of commonly discussed angles in [1]FCPs.

had formed. The [1.1]FCP $\mathbf{6_2}$ shows proton resonances of the α protons far apart at $\delta = 3.84$ and 5.21 ppm and those of the β protons in between over a narrow range at $\delta = 4.28$, 4.31, 4.39, and 4.48 ppm. This pattern is similar to other indium-bridged [1.1]FCPs, and can be best compared to the known species with the same bridging moiety $(Ar'Infc)_2$ ($\delta = 4.04$ (4 α-H), 4.45 (4 β-H), 4.53 (4 β-H), and 4.97 ppm (4 α-H))[18b] (see also discussion for $\mathbf{4_2}$ above). Even though only the Cp signals for the [1]FCP $\mathbf{6_1}$ could be assigned with certainty, there is no doubt that this species had formed. Compound $\mathbf{6_1}$ and the related gallium species **2** (ER_x = GaAr'; Scheme 1) show a similar signal pattern. Owing to the expectedly smaller tilt of the Cp ligands in $\mathbf{6_1}$ (angle α), the Cp signals are expected to cover a smaller chemical shift range, which was observed experimentally ($\mathbf{6_1}$: $\delta = 3.83$, 4.16 (α-H), 4.25, 4.29, 4.34, 4.53 (β-H) ppm; **2** (ER_x = GaAr'):[11] $\delta = 3.53$, 3.98 (α-H), 4.46, 4.50, 4.67, 4.70 ppm (β-H)). Further support for the interpretation of the NMR data came from a mass spectrum taken from the reaction mixture, which revealed the highest mass peak at $m/z = 1034.2$, clearly indicating the molecular ion of $\mathbf{6_2}$.

Molecular structures

To obtain structural information, DFT calculations were performed on the new inda[1]ferrocenophanes $\mathbf{4_1}$, $\mathbf{5_1}$, and $\mathbf{6_1}$. In particular, we intended to evaluate the influence of the *i*Pr groups on the ferrocene moiety and the *t*Bu groups on the aromatic ligand. We employed a similar tactic in the past for aluminum- and gallium-bridged [1]FCPs and [1]ruthenocenophanes equipped with the Mamx ligand.[13d] This study revealed that the *ortho*-*t*Bu group increased the strain of the [1]metallocenophanes on average by 5.5 kcal mol^{-1} (ΔH°_{298}). All of the DFT calculations were performed at the BP86/TZ2P level of theory, employing the ADF suite of programs (Experimental Section).[25] This method had been used in the past to reproduce structures of metallocenophanes successfully.[10b,13d,26] Figure 3 provides an overview of the calculated molecular structures, and selected structural data for all five species can be found in Table 1. First, the geometry of the recently prepared species **2** (ER_x = GaAr') was optimized and compared to the molecular structure, known from single-crystal X-ray analysis.[11] Furthermore, structures of the inda[1]ferrocenophanes $\mathbf{4_1}$, $\mathbf{5_1}$, $\mathbf{6_1}$, and **7** were optimized. These four [1]FCPs resulted from combining two bridging moieties, In(Mamx) and InAr', with two ferrocene units, $(H_4C_5)_2Fe$ (fc) and (S_p,S_p)-2,2'-$(i\text{PrH}_3C_5)_2Fe$ (fc^{iPr2}).

As it can be deduced from Table 1, the calculated values of species **2** (ER_x = GaAr') agree very well with the experimental data. From the set of angles commonly used to illustrate distortions in [1]FCPs (Figure 3),[27] small differences were found for the angles α and δ. For example, the calculated tilt angle of 15.19° is about 1° smaller than the measured angles of

Table 1. Calculated and measured angles [°] and bond lengths [Å] in [1]FCPs.[a]

	2		$\mathbf{4_1}$	$\mathbf{5_1}$	$\mathbf{6_1}$	**7**
ER_x	GaAr'		In(Mamx)	In(Mamx)	InAr'	InAr'
R/R' [a]	*i*Pr/H		H/*t*Bu	*i*Pr/*t*Bu	*i*Pr/H	H/H
	calcd	exptl[b,c]	calcd	calcd	calcd	calcd
α	15.19	16.26(9) 16.45(10)	11.44	11.42	10.96	11.18
β/β'	40.28/39.84	40.0(2)/39.1(2) 38.9(2)/38.4(2)	37.60/37.62	37.62/37.79	39.03/38.85	38.42/38.27
θ	93.76	93.44(10) 92.94(10)	86.24	86.12	87.49	87.08
δ	167.87	166.65(3) 166.78(3)	169.99	170.22	170.37	170.12
E–N	2.213	2.083(2) 2.102(2)	2.430	2.462	2.448	2.432
E–C1	1.989	1.971(3) 1.974(3)	2.195	2.212	2.178	2.177
E–C10	2.020	2.007(3) 2.009(3)	2.221	2.234	2.213	2.213
E–C20	2.017	2.014(2) 2.020(3)	2.221	2.227	2.214	2.209
Fe-E-C1	145.27	140.14(8) 143.93(7)	165.70	161.48	153.76	159.32
Fe-E-C1-C2	−25.25	−14.4(3) −22.1(4)	−17.76	−37.69	−24.69	−19.21

[a] See Figure 3. [b] Experimental data taken from reference [11]. [c] Two independent molecules were found in the asymmetric unit of **2**.

© 2014 Wiley-VCH Verlag GmbH & Co. KGaA, Weinheim

16.26(9) and 16.45(10)° (Table 1).[11,28] Such a difference is not worrisome. Differences of this magnitude are often found between crystallographically independent molecules in the solid state, indicating that a difference in the Cp tilt of 1° is not accompanied by a significant change in energy.[11,13b] Except for the Ga–N bond, other calculated bond lengths agree very well with the experimental values. The calculated Ga–N donor bond of 2.213 Å is longer than the measured Ga–N bond of 2.083(2) and 2.102(2).[11,26] A similar difference between calculated and measured values had been found for aluminum- or gallium-bridged sandwich compounds equipped with ligands capable of intramolecular donation.[13d] The difficulty of reproducing the donor bond length in our DFT calculations might have either to do with the flatness of the energy potential surface that allows for variations in the E–N distance without significant energy penalties, or is an effect of the polar environment in the crystal lattice that can decrease the E–N donor bond length.[29] Of course, both effects could be operative for species **2** (ER_x = GaAr′), resulting in an overestimation of the Ga–N bond lengths by 6% (average value).

Selected structural data for the four inda[1]ferrocenophanes $\mathbf{4_1}$, $\mathbf{5_1}$, $\mathbf{6_1}$, and **7** are listed in Table 1, and their molecular structures are illustrated in Figure 4. The amount of variation among the calculated Cp tilt angles is insignificantly small, with α being found in the range of 10.96 ($\mathbf{6_1}$) and 11.44° ($\mathbf{4_1}$). This magnitude of the tilting of the Cp rings in these [1]FCPs is expected based on the measured values for gallium-, germanium-, and tin-bridged species. For Group 14, descending from the 4th to the 5th period is accompanied by a decrease of tilt of around 5° (for example, α = 19.0(9) (Me_2Gefc),[30] 14.1(2) (tBu$_2$Snfc),[8b] 13.46(11) and 14.6(2)° (tBu$_2$Snfc^{iPr2}).[11] Because known tilt angles for gallium-bridged [1]FCPs are about 16° (α = 15.4(2) and 16.4(2)° [(Pytsi)Gafc],[13b] 15.83(19)° [(Me_2Ntsi)Gafc],[12b] 16.26(9) and 16.45(10)° [Ar′Gafc^{iPr2}]),[11] employing the 5° differential results in an expected α angle of 11° for inda[1]ferrocenophanes.

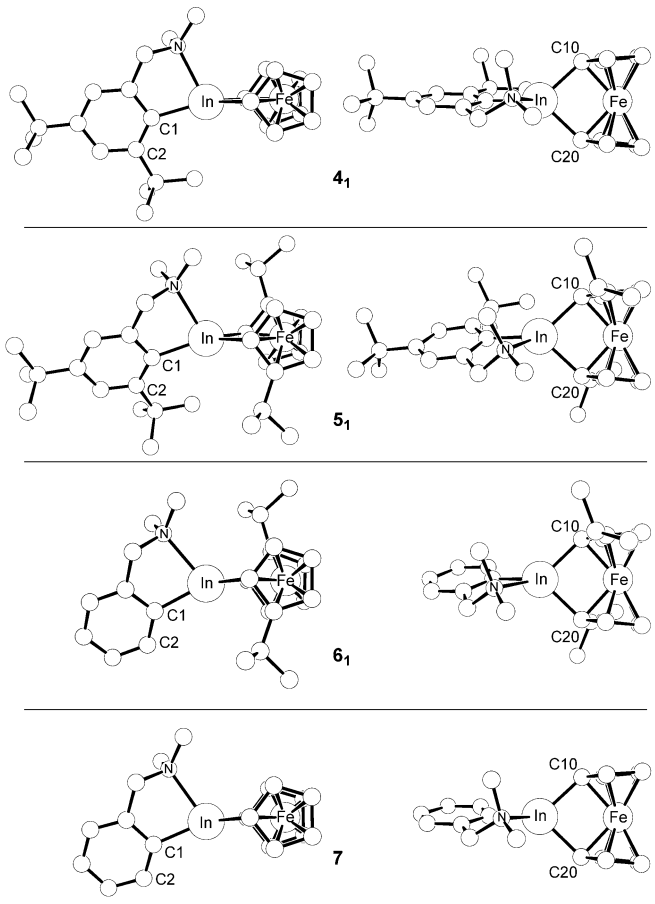

Figure 4. Calculated molecular structures of inda[1]ferrocenophanes $\mathbf{4_1}$, $\mathbf{5_1}$, $\mathbf{6_1}$, and **7**. Hydrogen atoms are omitted for clarity. Molecules are shown with views normal to the planes C10-Fe-C20 and Fe-In-C1, respectively.

The degree of steric congestion increases from species **7** to $\mathbf{5_1}$, with $\mathbf{4_1}$ and $\mathbf{6_1}$, equipped with either *t*Bu groups on the aromatic ligand ($\mathbf{4_1}$) or *i*Pr groups on ferrocene ($\mathbf{6_1}$), having an intermediate steric congestion (Figures 3 and 4). Comparing the bond lengths around indium shows that the most crowded species, compound $\mathbf{5_1}$, has the longest bonds. Within this group of four inda[1]ferrocenophanes, the differences between the shortest and the longest bonds are small: 0.032 (In–N), 0.035 (In–C1), 0.021 (In–C10), and 0.018 Å (In–C20), but could be the result of a "steric pressure" between the Mamx and the fc^{iPr2} moiety in $\mathbf{5_1}$.

For the aluminum- and gallium-bridged [1]FCPs and [1]ruthenocenophanes equipped with the Mamx ligand, DFT calculations revealed that the *ortho*-*t*Bu group of the Mamx moiety results in a "side shifting" of the entire ligand compared to species in which this *t*Bu group was substituted by a H atom.[13d] This shifting of the ligand can be illustrated by the M-E-C1 angle, which widened between 8.08 and 12.73° in species with the *ortho*-*t*Bu group of the known compounds.[13d] A similar but less-pronounced effect can be seen for the indium species (Figure 4): from **7** to $\mathbf{4_1}$, the Fe-In-C1 angle increases by 6.38°; from $\mathbf{6_1}$ to $\mathbf{5_1}$, the angle increases by 7.72° (Table 1). Comparing pairs of species that differ only in the presence or absence of *i*Pr groups reveals a decrease of the Fe-In-C1 angle by 4.22 ($\mathbf{4_1}$ to $\mathbf{5_1}$) and 5.56° (**7** to $\mathbf{6_1}$) when *i*Pr groups are present. Secondly, the tilt of the aromatic ligand relative to the ferrocene moiety changes depending on the steric congestion. This tilting can be illustrated by the torsion angle M-E-C1-C2, which increased between 5.26 and 6.98° by the presence of the *ortho*-*t*Bu group in the known strained [1]metallocenophanes of aluminum and gallium.[13d] For the new indium compounds, the *t*Bu groups either insignificantly influence the angle (1.45° for **7** to $\mathbf{4_1}$) or significantly increase the twist by 13.00° ($\mathbf{6_1}$ to $\mathbf{5_1}$). The effects of both alkyl groups combined make a significant difference for the tilting of the aromatic ligand: the non-substituted inda[1]ferrocenophane (**7**) compared with the highest substituted species ($\mathbf{5_1}$) reveals a difference in the Fe-In-C1-C2 angle of 18.48°. It is important to not over-interpret the importance of these structural changes. For example, the two crystallographically independent molecules of species **2** (ER_x = GaAr′) showed Fe-Ga-C1-C2 angles that differ by 7.7° (Table 1).

The structural effects of the alkyl groups can be summarized as follows: 1) The substitution pattern does not have a signifi-

© 2014 Wiley-VCH Verlag GmbH & Co. KGaA, Weinheim

cant influence on the tilting of Cp moieties (α angle) or other commonly used angles to describe [1]FCPs; 2) the *ortho*-*t*Bu group results in a widening of the Fe-E-C1 angle to an extent that is significantly smaller than that of similar aluminum and gallium species,[13d] which can be rationalized as In–C bonds are about 10% longer than Al-C or Ga–C bonds; thus, the *ortho*-*t*Bu group of the Mamx ligand is further removed from the ferrocene unit, resulting in reduced steric interactions; 3) the structural influence of the two *i*Pr groups on the ferrocene moiety ($\mathbf{6_1}$ compared to **7**) is similarly small as that of the *t*Bu groups on the Ar′ ligand ($\mathbf{4_1}$ compared to **7**); interestingly, both alkyl groups, *i*Pr and *t*Bu, result in an opposite effect with respect to the relative orientation of the aromatic ligand and the ferrocene moiety (angles Fe-In-C1 and Fe-In-C1-C2); and 4) the most distorted species is $\mathbf{5_1}$, evident by slightly elongated bonds of the fourfold-coordinated In atom, and by the extent of tilting of the Mamx ligand (Fe-E-C1-C2 = −37.69°).

Thermochemistry

The *i*Pr groups as well as the *t*Bu groups cause structural changes, triggering the question as to whether these groups also increase the strain of the [1]FCPs. Similar to our investigations of aluminum- and gallium-bridged species before,[13d] a hydrogenolysis reaction (Scheme 6) has been used to address this question. As listed in Table 2, for each inda[1]ferrocenophane $\Delta E^{(SCF)}$, ΔH^{o}_{298}, and ΔG^{o}_{298} were calculated (BP86/TZ2P; see Experimental Section for details). The absolute values are meaningless, as the hydrogenolysis is non-isodesmic. However, comparing two reactions that only differ in the presence or absence of one type of alkyl group (*i*Pr or *t*Bu) reveals the thermodynamic effect of this particular group; Table 3 provides data from these comparisons. Within this evaluation it is assumed that the alkyl groups do not have any influence on bonds that are formed or broken in the hydrogenolysis reaction.

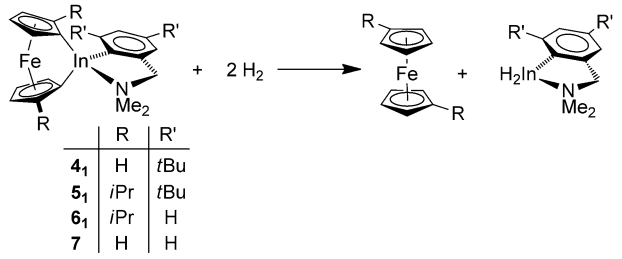

	R	R'
$\mathbf{4_1}$	H	*t*Bu
$\mathbf{5_1}$	*i*Pr	*t*Bu
$\mathbf{6_1}$	*i*Pr	H
7	H	H

Scheme 6. Hydrogenolysis reaction to evaluate strain in [1]FCPs.

Table 2. Thermodynamic data of the hydrogenolysis reaction.[a]

	R/R′	$\Delta E^{(SCF)}$	ΔH^{o}_{298}	ΔG^{o}_{298}
$\mathbf{4_1}$	H/*t*Bu	−40.46	−29.93	−25.46
$\mathbf{5_1}$	*i*Pr/*t*Bu	−43.57	−32.76	−30.42
$\mathbf{6_1}$	*i*Pr/H	−40.48	−28.37	−25.60
7	H/H	−39.62	−28.20	−23.74

[a] See Scheme 6. Values in kcal mol^{-1}.

Table 3. Effects of the *i*Pr and *ortho*-*t*Bu groups on the hydrogenolysis reaction.[a]

	Hydrogenolysis reactions of:	Effect of:	$\Delta\Delta E^{(SCF)}$	$\Delta\Delta H^{o}_{298}$	$\Delta\Delta G^{o}_{298}$
1	$\mathbf{4_1}$ compared to **7**	*t*Bu	−0.84	−1.72	−1.72
2	$\mathbf{5_1}$ compared to $\mathbf{6_1}$	*t*Bu	−3.09	−4.39	−4.82
3	$\mathbf{6_1}$ compared to **7**	*i*Pr	−0.86	−0.17	−1.86
4	$\mathbf{5_1}$ compared to $\mathbf{4_1}$	*i*Pr	−3.11	−2.83	−4.96

[a] See Scheme 6. Values in kcal mol^{-1}. Negative values indicate that species with alkyl groups result in a larger release of energy.

The thermodynamic data of two hydrogenolysis reactions are compared in such a way that a negative sign for the listed values in Table 3 indicates an increase of strain by one type of alkyl group. The fact that all values are negative reveals that in each case an increase of strain was found. Entries 1 and 2 in Table 3 show the effect of the *t*Bu groups, whereas entries 3 and 4 show effects caused by the *i*Pr groups. Furthermore, entry 1 shows the effect of the *t*Bu groups onto the fc moiety, whereas entry 2 shows the effect onto the fc^{iPr2} unit. Similarly, entry 3 shows the effect of the *i*Pr groups onto the Ar′ ligand, whereas entry 4 shows the effect onto the Mamx ligand. The sets of ΔΔ values are much smaller for entries 1 and 3 than for entries 2 and 4. This makes sense as entries 1 and 3 each show the effect of one type of alkyl group onto the non-bulky moiety (fc or Ar′); entries 2 and 4 each show the effect onto the bulky moiety (fc^{iPr2} or Mamx).

In summary, the order of strain effects from the smallest to the largest are: *i*Pr groups toward the Ar′ ligand (nearly no effect with $\Delta\Delta H^{o}_{298} = -0.17$ kcal mol^{-1}), followed by *t*Bu groups toward the fc moiety ($\Delta\Delta H^{o}_{298} = -1.72$ kcal mol^{-1}), followed by the *i*Pr groups toward the Mamx ligand ($\Delta\Delta H^{o}_{298} = -2.83$ kcal mol^{-1}), followed by the *t*Bu groups toward the Mamx ligand ($\Delta\Delta H^{o}_{298} = -4.39$ kcal mol^{-1}). This thermodynamic data are in agreement with the structural changes found for the indium-bridged [1]FCPs: species $\mathbf{5_1}$ is the most distorted [1]FCP and shows the strongest increase of strain by alkyl groups (−2.83 and −4.39 kcal mol^{-1}).

Conclusion

Salt-metathesis reactions between dilithioferrocene or the chiral isopropyl derivative Li_2fc^{iPr2} and the Ar′$InCl_2$ and (Mamx)$InCl_2$, respectively, gave the first inda[1]ferrocenophanes ($\mathbf{4_1}$, $\mathbf{5_1}$, $\mathbf{6_1}$; Schemes 3–5). For the cases where only either the stabilizing ligand at indium or the ferrocenediyl moiety was sterically demanding (Mamx or fc^{iPr2}), the targeted [1]FCP formed along with the unwanted [1.1]FCP. Only if bulky groups were used on the sandwich moiety as well as on the ligand at indium, the targeted [1]FCP ($\mathbf{5_1}$) formed exclusively. On the other hand, the known salt-metathesis reaction with bulky groups neither at the ferrocene unit nor at the ligand at indium only gave a [1.1]FCP [(Ar′Infc)$_2$].[18b] Such a preference of [1]FCPs over [1.1]FCPs by an increased steric demand of re-

© 2014 Wiley-VCH Verlag GmbH & Co. KGaA, Weinheim

agents in salt-metathesis reactions had been found for related aluminum- or gallium-bridged species before. For example, the formation of [1.1]FCPs could be suppressed for gallium species either by using the sterically demanding Mamx ligand or by using the bulky fc^{iPr2} moiety.[11,13c,d] For a given [1.1]FCP, the available space for a bridging moiety ER_x increases when ER_x is moved slightly away from the sandwich moiety by increased E–C bonds (Figure 1). Thus, with In–C bonds being around 10% longer than respective Al-C or Ga–C bonds, suppressing the formation of indium-bridged [1.1]FCPs requires bulky groups on both moieties: the sandwich and the ligand. These observations complement a failed attempt to prepare an inda[1]ferrocenophane by using the sterically demanding Me_2Ntsi ligand (Figure 2).[23] In contrast to aluminum and gallium, which yielded the respective [1]FCPs by employing this ligand,[12b] only the non-strained [1.1]FCP [(Me_2Ntsi)Infc]$_2$ was found for indium.[22]

DFT calculations on the observed inda[1]ferrocenophanes **4$_1$**, **5$_1$**, and **6$_1$** as well as on the hypothetical species **7** (Ar′Infc) revealed similar tilt angles α for all four species (10.96–11.44°; Table 1). Depending on the steric congestion, the relative orientation of the aromatic ligand with respect to the ferrocene unit changes significantly. These structural changes result from steric interactions between groups at the sandwich and ligand moieties and contribute significantly to the overall strain in [1]FCPs. The most pronounced effects were found for the sterically most encumbered inda[1]ferrocenophane **5$_1$**, with strain increases of -2.83 kcal mol^{-1} (effect of *i*Pr groups) and -4.39 kcal mol^{-1} (effect of *t*Bu groups), respectively. Attempts to isolate species **5$_1$** from reaction mixtures resulted in ROP to give the polymer **5$_n$**. This high reactivity was unexpected, as a tilt angle α of 11.42° is usually an expression of an insufficient amount of strain.[3a] We speculate that the increase of strain through steric interactions between the ferrocene and the ligand moieties is causing the increased reactivity. The reactivity of **5$_1$** is reminiscent of aluminum- and gallium-bridged [1]FCPs and [1]ruthenocenophanes equipped with the Mamx ligand, where a similar increase of strain by the presence of the *ortho*-*t*Bu group on the Mamx ligand had been revealed for the first time.[13c,d]

Experimental Section

General procedures

If not mentioned otherwise, all syntheses were carried out using standard Schlenk and glovebox techniques. Solvents were dried using an MBraun Solvent Purification System and stored under nitrogen over 3 Å molecular sieves. Methanol was degassed by bubbling nitrogen through it; water was removed by prolonged storage of methanol over 3 Å molecular sieves. All solvents for NMR spectroscopy were degassed (freeze–pump–thaw method) prior to use and stored under nitrogen over 3 Å molecular sieves. ^{1}H and ^{13}C NMR spectra were recorded on a 500 MHz Bruker Avance NMR spectrometer at 25 °C. ^{1}H chemical shifts were referenced to the residual protons of the deuterated solvents ($\delta = 7.15$ for C_6D_6; 7.26 ppm for $CDCl_3$); ^{13}C chemical shifts were referenced to the C_6D_6 signal at $\delta = 128.00$ ppm and the $CDCl_3$ signal at $\delta = 77.00$ ppm. Polymers **4$_n$** and **5$_n$** were isolated using inert gas techniques. Both materials can be handled under air for a short amount of time; however, overnight exposure of solutions of NMR samples of **4$_n$** or **5$_n$** to air resulted in intense signals of [$FeCp_2$] and [(*i*PrC_5H_4)$_2$Fe], respectively. Assignments for **4$_1$** and **4$_2$** were supported by additional NMR experiments (DEPT, HMQC, COSY). As signals of Cp protons show a fine structure, all signals were called multiplets. Mass spectra were measured on a VG 70SE and are reported in the form *m/z* (rel. intensity) [M^+], where *m/z* is the observed mass. The intensities are reported relative to the most-intense peak and [M^+] is the molecular-ion peak or a fragment; only characteristic mass peaks are listed. For the isotopic pattern, only the mass peak of the isotopologue or isotope with the highest natural abundance is listed. Elemental analyses were performed on a PerkinElmer 2400 CHN Elemental Analyzer using V_2O_5 to promote complete combustion.

Dynamic light scattering (DLS)

Dynamic light scattering experiments were performed using a nano series Malvern zetasizer instrument equipped with a 633 nm red laser. Samples were filtered through 0.2 μm syringe PTFE filters before they were analyzed in 1 cm glass cuvettes at concentrations of 5.0 and 2.5 mg mL^{-1} in thf at 25 °C. The refractive index of the polymers was assumed to be 1.5. For each polymer, two samples were prepared at each concentration. Every sample was measured three times. For poly(ferrocenyldimethylsilane) (PFS), the absolute molecular weights (M_w) in the range of 10 to 100 kDa and radii of gyration (R_g) are known.[24] Assuming that polymers **4$_n$** and **5$_n$** can be described as random coils, with thf being a good solvent, hydrodynamic radii R_h (**4$_n$**: 1.0 ± 0.1 nm; **5$_n$**: 2.4 ± 0.1 nm) gave radii of gyration (R_g) by using the equation $R_g/R_h = 2.05$.[31] Applying the published relation between log(R_g) and log(M_w) for poly(ferrocenyldimethylsilane) (PFS),[24] molecular weights were calculated (**4$_n$**: $M_w = 4.8 \pm 0.8$ kDa; **5$_n$**: $M_w = 24 \pm 2$ kDa; see the Supporting Information).

Reagents

The compounds Ar′$InCl_2$,[32] 6-(Me_2NCH_2)-2,4-*t*$Bu_2C_6H_2$Br (MamxBr),[13c] Li_2fc·tmeda,[33] and (S_p,S_p)-1,1′-dibromo-2,2′-diisopropylferrocene (**1**)[11] were prepared as described previously. Ferrocene (98%) and *n*BuLi (2.5 M in hexanes) was purchased from Sigma Aldrich; $InCl_3$ (99.9%) was purchased from Alpha Asaer. Silica gel 60 (EMD, Geduran, particle size 0.040–0.063 mm) was used for column chromatography and purchased from VWR.

Computational details

Calculations were carried out using the Amsterdam Density Functional package (version ADF2010.02).[25] The Slater-type orbital (STO) basis sets were of triple-ζ quality augmented with two polarization functions (ADF basis TZ2P). Core electrons were frozen (C, N 1s; Fe 2p; Ga 3d; In 4d) in our model of the electronic configuration for each atom. Relativistic effects were included by virtue of the zero order regular approximation (ZORA).[34] The local density approximation (LDA) by Vosko, Wilk, and Nusair (VWN)[35] was used together with the exchange correlation corrections of Becke[36] and Perdew[37] (BP86).[36,37] Tight optimization conditions were used for all compounds. Frequency calculations were used to confirm minima and provide thermodynamic information. The product of the hydrogenolysis reaction (Mamx)InH_2 (Scheme 6) showed a small imaginary frequency (-*i*27 cm^{-1}) corresponding to barrierless rotation of a *t*Bu group. The notation used for ΔH°_{298} and ΔG°_{298}

© 2014 Wiley-VCH Verlag GmbH & Co. KGaA, Weinheim

indicate standard condition ($p = 10^5$ Pa and $T = 298.15$ K). Graphical illustrations of calculated results were done with the help of *ORTEP-3 for Windows* (version 2.02);[38] extraction of structural parameters (see Table 1) from the calculated coordinates of [1]FCPs were done with the help of *Mercury* (version 3.1.1).[39]

Synthesis of [2,4-di-*tert*-butyl-6-{(dimethylamino)methyl}-phenyl]dichloroindigane, (Mamx)$InCl_2$ (3)

*n*BuLi (2.5 M in hexanes, 2.40 mL, 6.00 mmol) was added dropwise to a cold (−78 °C) solution of (Mamx)Br (1.80 g, 5.52 mmol) in Et_2O (20 mL). The reaction mixture was stirred at −78 °C for 1 h, resulting in a pale yellow solution, and added dropwise to a cold (0 °C) solution of $InCl_3$ (1.20 g, 5.43 mmol) in Et_2O (20 mL). The resulting mixture was warmed up to room temperature and stirred for 16 h, resulting in a pale green solution with a white precipitate. After the solid was filtered off, the pale green solution was concentrated to about 20 mL, and analytically pure product **3** was obtained as colorless crystals at about −80 °C (1.04 g, 44%). ^{1}H NMR (C_6D_6): $\delta =$ 1.30 (s, 9H, *t*Bu), 1.39 (s, 9H, *t*Bu), 1.90 (s, 6H, NMe_2), 2.89 (s, 2H, CH_2), 6.74 (s, 1H, C_6H_2), 7.57 (s, 1H, C_6H_2) ppm; ^{13}C NMR (C_6D_6): $\delta =$ 31.46 [C(CH_3)$_3$], 32.47 [C(CH_3)$_3$], 34.88 [*C*(CH_3)$_3$], 35.84 [*C*(CH_3)$_3$], 45.28 (NMe_2), 65.61 (CH_2), 121.79 (C-5), 123.73 (C-3), 141.35 (C-6), 152.62 (C-4), 158.54 ppm (C-2) (Note: The *ipso*-C-In was not detected. Assignments are supported by a DEPT measurement and are carried out in analogy to the known compound (Mamx)$GaCl_2$; see Ref. [13c]); MS (70 eV): *m/z* (%): 431 (9) [M^+], 396 (21) [M^+−Cl], 245 (100) [$C_{17}H_{27}N^+$], 203 (78) [$C_{15}H_{23}^+$], 58 (39) [$C_4H_{10}^+$]; HRMS (70 eV): calcd for $C_{17}H_{28}Cl_2InN$: 431.0638; found: 431.0624; elemental analysis calcd (%) for $C_{17}H_{28}Cl_2InN$ (432.135): C 47.25, H 6.53, N 3.24; found: C 47.33, H 6.57, N 3.19.

Synthesis of 4_1, 4_2, and 4_n

A solution of **3** (0.935 g, 2.16 mmol) in Et_2O (45 mL) was added dropwise to a slurry of [(LiC_5H_4)$_2$Fe·tmeda] (0.681 g, 2.17 mmol) in Et_2O (20 mL). The reaction mixture was stirred at room temperature for 5 h, resulting in a red solution with a white precipitate. After the solid was filtered off, the red solution was kept at −78 °C for 48 h, which resulted in an orange precipitate and a red solution. The precipitate was filtered off, washed with hexanes (3×10 mL), and dried under vacuum to give $\mathbf{4_2}$ (0.273 g, 23%) together with small amounts of impurities. All of the volatiles were removed from the red mother liquor to give a red paste. This paste was dissolve in toluene (5 mL) and added dropwise to hexanes while being stirred vigorously. An orange-red precipitate and an orange solution were obtained. The precipitate was filtered off, washed with cold (−20 °C) hexanes (3×10 mL), and dried under vacuum to give $\mathbf{4_1}$ (0.219 g, 19%) together with small amounts of impurities. All of the volatiles were removed from the orange mother liquor to give an orange paste. This paste was dissolve in toluene (5 mL) and added dropwise to MeOH (30 mL) while being stirred vigorously. An orange precipitate and a pale orange solution were obtained. The precipitate was filtered off, washed with MeOH (3× 15 mL), and dried under vacuum to give $\mathbf{4_n}$ (0.378 g, 32%). Note that crystallization attempts for $\mathbf{4_1}$ and $\mathbf{4_2}$ from a variety of organic solvents (thf, CH_2Cl_2, toluene) at different temperatures, including layering solutions with hexanes, did not result in crystalline compounds.

Inda[1]ferrocenophane $\mathbf{4_1}$: ^{1}H NMR (C_6D_6): $\delta = 1.40$ (s, 9H, *t*Bu), 1.60 (s, 9H, *t*Bu), 2.16 (s, 6H, NMe_2), 3.33 (s, 2H, CH_2), 4.22 (m, 2H, CH-α of Cp), 4.39 (m, 2H, CH-α of Cp), 4.41 (m, 2H, CH-β of Cp), 4.46 (m, 2H, CH-β of Cp), 7.00 (s, 1H, C_6H_2), 7.67 (s, 1H, C_6H_2) ppm; ^{13}C NMR (C_6D_6): $\delta =$ 31.80 [C(CH_3)$_3$], 33.16 [C(CH_3)$_3$], 34.72 [*C*(CH_3)$_3$], 36.93 [*C*(CH_3)$_3$], 46.24 (NMe_2), 68.84 (CH_2), 70.13, 70.53, 75.54, 76.96 (Cp), 120.49, 121.87, 143.94, 149.17, 159.50 (C_6H_2) ppm (Note: The *ipso*-C-In was not detected); MS (70 eV): *m/z* (%): 545 (13) [M^+], 515 (31), 432 (25) [$C_{19}H_{19}FeInN^+$], 184 (62) [$C_{10}H_8Fe^+$], 121 (100) [$C_5H_5Fe^+$]; HRMS (70 eV): *m/z* calcd for $C_{27}H_{36}FeInN$: 545.1236; found: 545.1249; elemental analysis calcd (%) for $C_{27}H_{36}FeInN$ (545.244): C 59.48, H 6.65, N 2.57; found: C 58.58, H 6.58, N 2.46 (Note: Species $\mathbf{4_1}$ contained small amounts of unknown impurities; see the Supporting Information for NMR spectra).

Diinda[1.1]ferrocenophane $\mathbf{4_2}$: ^{1}H NMR ($CDCl_3$): $\delta = 1.35$ (s, 18H, *t*Bu), 1.74 (s, 18H, *t*Bu), 1.95 (s, 12H, NMe_2), 3.45 (s, 4H, CH_2), 3.91 (m, 4H, CH-α of Cp), 4.26 (m, 8H, CH-β of Cp), 4.40 (m, 4H, CH-α of Cp), 6.90 (s, 2H, C_6H_2), 7.50 ppm (s, 2H, C_6H_2) (Note: Due to the poor solubility of $\mathbf{4_2}$ in organic solvents, the ^{13}C NMR spectrum had a high noise level; see the Supporting Information); ^{13}C NMR ($CDCl_3$): $\delta =$ 31.56 [C(CH_3)$_3$], 33.06 [C(CH_3)$_3$], 34.62 [*C*(CH_3)$_3$], 36.29 [*C*(CH_3)$_3$], 45.30 (NMe_2), 67.42 (CH_2), 69.34 (C-β of Cp), 69.38 (C-β of Cp), 75.13 (C-α of Cp), 75.89 (*ipso*-C of Cp, tentative), 76.84 (C-α of Cp), 120.49, 120.55, 144.49, 149.05, 158.68 ppm (C_6H_2); MS (70 eV): *m/z* (%): 1090 (9) [M^+], 731 (17) [$C_{37}H_{46}Fe_2InN^+$], 626 (20) [$C_{24}H_{24}FeIn_2N_2^+$], 581 (100) [$C_{23}H_{19}FeIn_2^+$], 546 (36) [$C_{27}H_{37}FeInN^+$], 425 (17) [$C_{22}H_{32}InN^+$], 247 (34) [$C_9H_{10}InN^+$], 186 (87) [$C_{10}H_{10}Fe^+$]; HRMS (70 eV): *m/z* calcd for $C_{54}H_{72}Fe_2In_2N_2$: 1090.2472; found: 1090.2481; elemental analysis calcd (%) for $C_{54}H_{72}Fe_2In_2N_2$ (1090.489): C 59.48, H 6.65, N 2.57; found: C 58.00, H 6.44, N 2.43 (Note: Species $\mathbf{4_2}$ contained small amounts of unknown impurities; see the Supporting Information for NMR spectra).

Poly(ferrocenylindigane) $\mathbf{4_n}$: ^{1}H NMR (C_6D_6): $\delta =$ 1.24–1.38 (m, 9H, *t*Bu), 1.48–1.66 (m, 9H, *t*Bu), 2.15–2.77 (m, 6H, NMe_2), 3.40–3.69 (m, 2H, CH_2), 3.84–4.62 (m, 8H, Cp), 6.86–7.04 (m, 1H, C_6H_2), 7.38–7.55 (m, 1H, C_6H_2) ppm.

Poly(ferrocenylindigane) $\mathbf{5_n}$

*n*BuLi (2.5 M in hexanes, 0.85 mL, 2.1 mmol) was added dropwise to a cold (0 °C) solution of **1** (0.432 g, 1.01 mmol) in a mixture of thf (1 mL) and hexanes (9 mL). The reaction mixture was stirred at 0 °C for 30 min, resulting in an orange solution. A solution of **3** (0.438 g, 1.01 mmol) in Et_2O (20 mL; room temperature) was added dropwise within 1 min to the solution. The resulting reaction mixture was warmed to room temperature and stirred for 30 min, resulting in a red solution with a white precipitate. All of the volatiles were removed under vacuum, yielding a red solid. Et_2O (25 mL) was added to the red solid and the mixture was stirred for 30 min, yielding a red solution with a white precipitate. The solid was filtered off and the filtrate was stirred for 3 h, resulting in an orange-red solution with orange gelatinous material. All of the volatiles were removed under vacuum, yielding an orange-red paste, which was dissolved in toluene (5 mL). The toluene solution was added dropwise to hexanes (20 mL), which was stirred vigorously, yielding an orange precipitate with a red solution. The precipitate (0.438 g) was filtered off, washed with hexanes (3×5 mL), and dried under vacuum to give poly(ferrocenylindigane) $\mathbf{5_n}$ (0.211 g, 33%). ^{1}H NMR (C_6D_6): $\delta =$ 1.24–1.38 (br peaks, 9H, *t*Bu), 1.48–1.66 (br m, 9H, *t*Bu), 2.15–2.77 (br m, 6H, NMe_2), 3.40–3.69 (m, 2H, CH_2), 3.84–4.62 (m, 8H, Cp), 6.86–7.04 (m, 1H, C_6H_2), 7.38–7.55 (m, 1H, C_6H_2) ppm.

Identification of the inda[1]ferrocenophane $\mathbf{5_1}$

Inda[1]ferrocenophane $\mathbf{5_1}$ is an intermediate in the preparation of $\mathbf{5_n}$ and was identified by ^{1}H NMR spectroscopy. All attempts to isolate pure inda[1]ferrocenophane $\mathbf{5_1}$ were unsuccessful. ^{1}H NMR (C_6D_6; taken from an aliquot of the reaction mixture after 30 min): $\delta =$ 1.16 (d, 3H, CHMe_2), 1.19 (d, 3H, CHMe_2), 1.39 (s, 9H, *t*Bu), 1.50

© 2014 Wiley-VCH Verlag GmbH & Co. KGaA, Weinheim

(d, 3H, CH*Me*$_2$), 1.53 (d, 3H, CH*Me*$_2$), 1.65 (s, 9H, *t*Bu), 1.91 (s, 3H, NMe$_2$), 2.30 (s, 3H, CH$_3$ of NMe$_2$), 2.38 (sept, 1H, C*H*Me$_2$), 2.65 (d, 1H, CH$_2$), 2.86 (sept, 1H, C*H*Me$_2$), 3.68 (m, 1H, CH-α of Cp), 3.94 (d, 1H, CH$_2$), 4.11 (m, 1H, CH-α of Cp), 4.47 (m, 1H, CH-β of Cp), 4.50, (m, 1H, CH-β of Cp) 4.67 (m, 1H, CH-β of Cp), 4.73 (m, 1H, CH-β of Cp), 6.93 (s, 1H, C$_6$H$_2$), 7.71 (s, 1H, C$_6$H$_2$) ppm; ^{13}C NMR (C$_6$D$_6$): $\delta =$ 21.74 [CH(*C*H$_3$)$_2$], 22.73 [CH(CH$_3$)$_2$], 28.07 [CH(*C*H$_3$)$_2$], 28.14 [CH(*C*H$_3$)$_2$], 31.67 [C(*C*H$_3$)$_3$], 32.15 [CH(CH$_3$)$_2$], 32.82 [*C*H(CH$_3$)$_2$], 33.11 [C(*C*H$_3$)$_3$], 34.81 [*C*(CH$_3$)$_3$], 36.54 [*C*(CH$_3$)$_3$]„ 44.46 (NMe$_2$), 48.28 (NMe$_2$), 50.53, 52.28 (*ipso*-Cp, In, tentative), 69.18 (CH$_2$), 69.73 (C-β of Cp), 69.93 (C-β of Cp), 74.31 (C-β of Cp), 74.86 (C-β of Cp), 80.84 (C-α of Cp), 80.89 (C-α of Cp), 104.33 (*ipso*-Cp, *i*Pr), 105.69 (*ipso*-Cp, *i*Pr), 121.44, 122.23, 128.51, 143.63, 150.45, 159.64 (C$_6$H$_2$) ppm. Note: The *ipso*-C-In was not detected. Assignments were carried ou along the lines of the known gallium compound **2**.[11]

Synthesis of a mixture of 6_1 and 6_2

*n*BuLi (2.5 m in hexanes, 0.86 mL, 2.2 mmol) was added dropwise to a cold (0 °C) solution of **1** (0.437 g, 1.02 mmol) in a mixture of thf (1 mL) and hexanes (9 mL). The reaction mixture was stirred at 0 °C for 30 min, resulting in an orange solution. A solution of Ar′InCl$_2$ (0.340 g, 1.06 mmol) in Et$_2$O (20 mL; room temperature) was added dropwise within 1 min to the solution. The cold bath was removed after 5 min and the color of the reaction mixture changed from orange to light-red along with a formation of a colorless precipitate. The reaction was stirred for another 5 min, all volatiles were removed, and the resulting red residue was dissolved in hexanes (10 mL). After removal of all solids through filtration, solvent was removed under vacuum. The mixture was analyzed by ^{1}H NMR spectroscopy and MS. As many signals overlap with other smaller signals, the measured intensities are imprecise. The signals for the aromatic protons above 8 ppm do not overlap significantly with other peaks and were therefore used to calculate the approximate molar ratio of 0.86:1.0 for **6$_1$**:**6$_2$**. As the intensity of the peaks for species **6$_1$** is about half of that of respective peaks of species **6$_2$**; only certain peaks could be assigned for **6$_1$**. ^{1}H NMR (C$_6$D$_6$) for **6$_2$**: $\delta =$ 1.08 (d, 6H, CH*Me*$_2$, tentative), 1.21 (d, 6H, CH*Me*$_2$, tentative), 1.24 (d, 6H, CH*Me*$_2$, tentative), 1.60 (d, 6H, CH*Me*$_2$, tentative), 1.65 (s, 6H, NMe$_2$), 2.12 (s, 6H, NMe$_2$), 2.41 (sept, 2H, C*H*Me$_2$), 3.22 (d, 2H, CH$_2$), 3.34 (sept, 2H, C*H*Me$_2$), 3.59 (d, 2H, CH$_2$), 3.85 (m, 2H, CH-α of Cp), 4.28 (m, 2H, CH-β of Cp), 4.31 (m, 2H, CH-β of Cp), 4.39 (m, 2H, CH-β of Cp), 4.49 (m, 2H, CH-β of Cp), 5.22 (m, 2H, CH-α of Cp), 7.02 (d, 2H, Ar), 7.22 (t, 2H, Ar), 7.42 (t, 2H, Ar), 8.36 (d, 2H, Ar); ^{1}H NMR (C$_6$D$_6$) for **6$_1$** (partial assignment): $\delta =$ 3.83 (m, 2H, CH-α of Cp), 4.16 (m, 2H, CH-α of Cp), 4.25 (m, 2H, CH-β of Cp), 4.29 (m, 2H, CH-β of Cp), 4.34 (m, 2H, CH-β of Cp), 4.53 (m, 2H, CH-β of Cp), 8.49 (d, 2H, Ar). MS (70 eV) of the reaction mixture showed the highest peak at *m/z* at 1034.2 (M$^+$ of **6$_2$**).

Acknowledgements

We thank the Natural Sciences and Engineering Research Council of Canada (NSERC Discovery Grant, J.M.) for support. We thank the Canada Foundation for Innovation (CFI) and the government of Saskatchewan for funding of the NMR facilities in the Saskatchewan Structural Sciences Centre (SSSC). We thank Prof. Ildiko Badea (University of Saskatchewan, College of Pharmacy and Nutrition) and Prof. Ian Burgess (University of Saskatchewan, Department of Chemistry) for making instruments available for our studies.

Keywords: density functional calculations · ferrocenophanes · indium · metallocenes · ring-opening polymerization

[1] Selected reviews on metallopolymers and ROP of strained sandwich compounds: a) I. Manners, *Adv. Mater.* **1994**, *6*, 68–71; b) I. Manners, *Science* **2001**, *294*, 1664–1666; c) I. Manners, *Synthetic Metal-Containing Polymers*, Wiley-VCH, Weinheim, **2004**; d) V. Bellas, M. Rehahn, *Angew. Chem.* **2007**, *119*, 5174–5197; *Angew. Chem. Int. Ed.* **2007**, *46*, 5082–5104; e) V. Marin, E. Holder, R. Hoogenboom, U. S. Schubert, *Chem. Soc. Rev.* **2007**, *36*, 618–635; f) G. R. Whittell, I. Manners, *Adv. Mater.* **2007**, *19*, 3439–3468; g) K. A. Williams, A. J. Boydston, C. W. Bielawski, *Chem. Soc. Rev.* **2007**, *36*, 729–744; h) J. C. Eloi, L. Chabanne, G. R. Whittell, I. Manners, *Mater. Today* **2008**, *11*, 28–36; i) M. A. Hempenius, C. Cirmi, F. Lo Savio, J. Song, G. J. Vancso, *Macromol. Rapid Commun.* **2010**, *31*, 772–783; j) W. Y. Wong, P. D. Harvey, *Macromol. Rapid Commun.* **2010**, *31*, 671–713; k) R. A. Krüger, T. Baumgartner, *Dalton Trans.* **2010**, *39*, 5759–5767; l) G. R. Whittell, M. D. Hager, U. S. Schubert, I. Manners, *Nat. Mater.* **2011**, *10*, 176–188.

[2] a) J. A. Massey, K. Temple, L. Cao, Y. Rharbi, J. Raez, M. A. Winnik, I. Manners, *J. Am. Chem. Soc.* **2000**, *122*, 11577–11584; b) L. Cao, I. Manners, M. A. Winnik, *Macromolecules* **2002**, *35*, 8258–8260; c) H. Wang, W. Lin, K. P. Fritz, G. D. Scholes, M. A. Winnik, I. Manners, *J. Am. Chem. Soc.* **2007**, *129*, 12924–12925; d) X. S. Wang, G. Guerin, H. Wang, Y. S. Wang, I. Manners, M. A. Winnik, *Science* **2007**, *317*, 644–647; e) T. Gädt, N. S. Ieong, G. Cambridge, M. A. Winnik, I. Manners, *Nat. Mater.* **2009**, *8*, 144–150; f) J. B. Gilroy, T. Gädt, G. R. Whittell, L. Chabanne, J. M. Mitchels, R. M. Richardson, M. A. Winnik, I. Manners, *Nat. Chem.* **2010**, *2*, 566–570; g) A. Presa Soto, J. B. Gilroy, M. A. Winnik, I. Manners, *Angew. Chem.* **2010**, *122*, 8396–8399; *Angew. Chem. Int. Ed.* **2010**, *49*, 8220–8223; h) T. Gädt, F. H. Schacher, N. McGrath, M. A. Winnik, I. Manners, *Macromolecules* **2011**, *44*, 3777–3786; i) J. B. Gilroy, S. K. Patra, J. M. Mitchels, M. A. Winnik, I. Manners, *Angew. Chem.* **2011**, *123*, 5973–5977; *Angew. Chem. Int. Ed.* **2011**, *50*, 5851–5855; j) F. He, T. Gädt, I. Manners, M. A. Winnik, *J. Am. Chem. Soc.* **2011**, *133*, 9095–9103; k) S. K. Patra, R. Ahmed, G. R. Whittell, D. J. Lunn, E. L. Dunphy, M. A. Winnik, I. Manners, *J. Am. Chem. Soc.* **2011**, *133*, 8842–8845; l) J. Qian, G. Guerin, Y. Lu, G. Cambridge, I. Manners, M. A. Winnik, *Angew. Chem.* **2011**, *123*, 1660–1663; *Angew. Chem. Int. Ed.* **2011**, *50*, 1622–1625; m) P. A. Rupar, G. Cambridge, M. A. Winnik, I. Manners, *J. Am. Chem. Soc.* **2011**, *133*, 16947–16957; n) P. A. Rupar, L. Chabanne, M. A. Winnik, I. Manners, *Science* **2012**, *337*, 559–562; o) H. Qiu, G. Cambridge, M. A. Winnik, I. Manners, *J. Am. Chem. Soc.* **2013**, *135*, 12180–12183.

[3] Recent reviews on strained sandwich compounds: a) D. E. Herbert, U. F. J. Mayer, I. Manners, *Angew. Chem.* **2007**, *119*, 5152–5173; *Angew. Chem. Int. Ed.* **2007**, *46*, 5060–5081; b) M. Tamm, *Chem. Commun.* **2008**, 3089–3100; c) H. Braunschweig, T. Kupfer, *Acc. Chem. Res.* **2010**, *43*, 455–465; d) R. A. Musgrave, A. D. Russell, I. Manners, *Organometallics* **2013**, *32*, 5654–5667.

[4] a) R. Rulkens, A. J. Lough, I. Manners, *J. Am. Chem. Soc.* **1994**, *116*, 797–798; b) Y. Z. Ni, R. Rulkens, I. Manners, *J. Am. Chem. Soc.* **1996**, *118*, 4102–4114.

[5] N. S. Ieong, I. Manners, *Macromol. Chem. Phys.* **2009**, *210*, 1080–1086.

[6] For anionic ROP, see: a) C. H. Honeyman, T. J. Peckham, J. A. Massey, I. Manners, *Chem. Commun.* **1996**, 2589–2590; b) T. J. Peckham, J. A. Massey, C. H. Honeyman, I. Manners, *Macromolecules* **1999**, *32*, 2830–2837.

[7] For photocontrolled ROP, see: a) T. Mizuta, M. Onishi, K. Miyoshi, *Organometallics* **2000**, *19*, 5005–5009; b) T. Mizuta, Y. Imamura, K. Miyoshi, *J. Am. Chem. Soc.* **2003**, *125*, 2068–2069; c) S. K. Patra, G. R. Whittell, S. Nagiah, C.-L. Ho, W.-Y. Wong, I. Manners, *Chem. Eur. J.* **2010**, *16*, 3240–3250.

[8] For examples the chemistry of stanna[1]ferrocenophanes, see: a) R. Rulkens, A. J. Lough, I. Manners, *Angew. Chem.* **1996**, *108*, 1929–1931; *Angew. Chem. Int. Ed. Engl.* **1996**, *35*, 1805–1807; b) F. Jäkle, R. Rulkens, G. Zech, D. A. Foucher, A. J. Lough, I. Manners, *Chem. Eur. J.* **1998**, *4*, 2117–2128; c) H. K. Sharma, F. Cervantes-Lee, J. S. Mahmoud, K. H. Pannell, *Organometallics* **1999**, *18*, 399–403; d) F. Jäkle, R. Rulkens, G. Zech, J. Massey, I. Manners, *J. Am. Chem. Soc.* **2000**, *122*, 4231–4232; e) T.

 © 2014 Wiley-VCH Verlag GmbH & Co. KGaA, Weinheim

Baumgartner, F. Jäkle, R. Rulkens, G. Zech, A. J. Lough, I. Manners, *J. Am. Chem. Soc.* **2002**, *124*, 10062 – 10070.

[9] For example, bora[1]ferrocenophanes were polymerized thermally, but the resulting polymeric materials were insoluble in organic solvents; see Ref. [10].

[10] a) H. Braunschweig, R. Dirk, M. Müller, P. Nguyen, R. Resendes, D. P. Gates, I. Manners, *Angew. Chem.* **1997**, *109*, 2433 – 2435; *Angew. Chem. Int. Ed. Engl.* **1997**, *36*, 2338 – 2340; b) A. Berenbaum, H. Braunschweig, R. Dirk, U. Englert, J. C. Green, F. Jäkle, A. J. Lough, I. Manners, *J. Am. Chem. Soc.* **2000**, *122*, 5765 – 5774.

[11] S. Sadeh, G. Schatte, J. Müller, *Chem. Eur. J.* **2013**, *19*, 13408 – 13417.

[12] a) J. A. Schachner, C. L. Lund, J. W. Quail, J. Müller, *Organometallics* **2005**, *24*, 785 – 787; b) C. L. Lund, J. A. Schachner, J. W. Quail, J. Müller, *Organometallics* **2006**, *25*, 5817 – 5823; c) J. A. Schachner, S. Tockner, C. L. Lund, J. W. Quail, M. Rehahn, J. Müller, *Organometallics* **2007**, *26*, 4658 – 4662; d) N. C. Breit, T. Ancelet, J. W. Quail, G. Schatte, J. Müller, *Organometallics* **2011**, *30*, 6150 – 6158.

[13] a) J. A. Schachner, C. L. Lund, J. W. Quail, J. Müller, *Organometallics* **2005**, *24*, 4483 – 4488; b) J. A. Schachner, J. W. Quail, J. Müller, *Acta Crystallogr. Sect. E* **2008**, *64*, m 517; c) B. Bagh, J. B. Gilroy, A. Staubitz, J. Müller, *J. Am. Chem. Soc.* **2010**, *132*, 1794 – 1795; d) B. Bagh, G. Schatte, J. C. Green, J. Müller, *J. Am. Chem. Soc.* **2012**, *134*, 7924 – 7936.

[14] For recent applications of the flytrap route, see: a) H. Braunschweig, F. Seeler, R. Sigritz, *J. Organomet. Chem.* **2007**, *692*, 2354 – 2356; b) D. E. Herbert, U. F. J. Mayer, J. B. Gilroy, M. J. Lopez-Gomez, A. J. Lough, J. P. H. Charmant, I. Manners, *Chem. Eur. J.* **2009**, *15*, 12234 – 12246; c) D. E. Herbert, J. B. Gilroy, A. Staubitz, M. F. Haddow, J. N. Harvey, I. Manners, *J. Am. Chem. Soc.* **2010**, *132*, 1988 – 1998; d) J. B. Gilroy, A. D. Russell, A. J. Stonor, L. Chabanne, S. Baljak, M. F. Haddow, I. Manners, *Chem. Sci.* **2012**, *3*, 830 – 841.

[15] It can be assumed that these insoluble products are oligomers or polymers and not the targeted FCPs. Based on our recent results, we speculate that oligomers were formed through polycondensation reactions; see Ref. [11].

[16] For the preparation of boron-bridged polyferrocenes through unusual redistribution/polycondensation reactions, see: a) J. B. Heilmann, M. Scheibitz, Y. Qin, A. Sundararaman, F. Jäkle, T. Kretz, M. Bolte, H. W. Lerner, M. C. Holthausen, M. Wagner, *Angew. Chem.* **2006**, *118*, 934 – 939; *Angew. Chem. Int. Ed.* **2006**, *45*, 920 – 925; b) J. B. Heilmann, Y. Qin, F. Jäkle, H. W. Lerner, M. Wagner, *Inorg. Chim. Acta* **2006**, *359*, 4802 – 4806; c) M. Scheibitz, H. Y. Li, J. Schnorr, A. S. Perucha, M. Bolte, H. W. Lerner, F. Jäkle, M. Wagner, *J. Am. Chem. Soc.* **2009**, *131*, 16319 – 16329.

[17] For the formation of a Me_2B-bridged [1.1]FCP, see: M. Scheibitz, R. F. Winter, M. Bolte, H.-W. Lerner, M. Wagner, *Angew. Chem.* **2003**, *115*, 954 – 957; *Angew. Chem. Int. Ed.* **2003**, *42*, 924 – 927.

[18] a) H. Braunschweig, C. Burschka, G. K. B. Clentsmith, T. Kupfer, K. Radacki, *Inorg. Chem.* **2005**, *44*, 4906 – 4908; b) J. A. Schachner, G. A. Orlowski, J. W. Quail, H.-B. Kraatz, J. Müller, *Inorg. Chem.* **2006**, *45*, 454 – 459; c) C. L. Lund, J. A. Schachner, I. J. Burgess, J. W. Quail, G. Schatte, J. Müller, *Inorg. Chem.* **2008**, *47*, 5992 – 6000; d) B. Bagh, N. C. Breit, K. Harms, G. Schatte, I. J. Burgess, H. Braunschweig, J. Müller, *Inorg. Chem.* **2012**, *51*, 11155 – 11167.

[19] For a recent overview of non-carbon bridged [1.1]FCPs, see Ref. [18d]. For unsymmetrically bridged [1.1]FCPs, see: a) B. Bagh, N. C. Breit, S. Dey, J. B. Gilroy, G. Schatte, K. Harms, J. Müller, *Chem. Eur. J.* **2012**, *18*, 9722 – 9733; b) B. Bagh, N. C. Breit, J. B. Gilroy, G. Schatte, J. Müller, *Chem. Commun.* **2012**, *48*, 7823 – 7825.

[20] Mamx stands for methylaminomethyl-*m*-xylyl; see: M. Yoshifuji, K. Kamijo, K. Toyota, *Tetrahedron Lett.* **1994**, *35*, 3971 – 3974.

[21] The Mamx ligand is comparable to the 2,4,6-tri-*tert*-butylphenyl (Mes*) ligand. Mes*$InCl_2$ is a monomer in the solid state; see: a) S. Schulz, S. Pusch, E. Pohl, S. Dielkus, R. Herbst-Irmer, A. Meller, H. W. Roesky, *Inorg. Chem.* **1993**, *32*, 3343 – 3346; b) M. A. Petrie, P. P. Power, H. V. R. Dias, K. Ruhlandt-Senge, K. M. Waggoner, R. J. Wehmschulte, *Organometallics* **1993**, *12*, 1086 – 1093.

[22] J. A. Schachner, C. L. Lund, I. J. Burgess, J. W. Quail, G. Schatte, J. Müller, *Organometallics* **2008**, *27*, 4703 – 4710.

[23] As all of the reported aluminum-, gallium-, and indium-bridged [1.1]FCPs exist as *anti*-isomers in the solid state, species $\mathbf{4_2}$ is expected to also be an *anti*-isomer; see Ref. [18d] and cited references.

[24] J. A. Massey, K. Kulbaba, M. A. Winnik, I. Manners, *J. Polym. Sci. Part B* **2000**, *38*, 3032 – 3041.

[25] a) E. J. Baerends, D. E. Ellis, P. Ros, *Chem. Phys.* **1973**, *2*, 41 – 51; b) L. Versluis, T. Ziegler, *J. Chem. Phys.* **1988**, *88*, 322 – 328; c) G. te Velde, E. J. Baerends, *J. Comput. Phys.* **1992**, *99*, 84 – 98; d) C. F. Fonseca Guerra, J. G. Snijders, G. te Velde, E. J. Baerends, *Theor. Chem. Acc.* **1998**, *99*, 391 – 403.

[26] a) I. Matas, G. R. Whittell, B. M. Partridge, J. P. Holland, M. F. Haddow, J. C. Green, I. Manners, *J. Am. Chem. Soc.* **2010**, *132*, 13279 – 13289; b) G. Masson, D. E. Herbert, G. R. Whittell, J. P. Holland, A. J. Lough, J. C. Green, I. Manners, *Angew. Chem.* **2009**, *121*, 5061 – 5064; *Angew. Chem. Int. Ed.* **2009**, *48*, 4961 – 4964; c) S. Barlow, M. J. Drewitt, T. Dijkstra, J. C. Green, D. O'Hare, C. Whittingham, H. H. Wynn, D. P. Gates, I. Manners, J. M. Nelson, J. K. Pudelski, *Organometallics* **1998**, *17*, 2113 – 2120.

[27] M. Herberhold, *Angew. Chem.* **1995**, *107*, 1985 – 1987; *Angew. Chem. Int. Ed. Engl.* **1995**, *34*, 1837 – 1839.

[28] Two crystallographically independent molecules were found in the asymmetric unit.

[29] For simple Lewis acid – base adducts, large differences between gas-phase and solid-state molecular structures were found; see: J. Müller, U. Ruschewitz, O. Indris, H. Hartwig, W. Stahl, *J. Am. Chem. Soc.* **1999**, *121*, 4647 – 4652, and references therein.

[30] D. A. Foucher, M. Edwards, R. A. Burrow, A. J. Lough, I. Manners, *Organometallics* **1994**, *13*, 4959 – 4966.

[31] W. Burchard in *Branched Polymers II, Vol. 143*, **1999**, pp. 113 – 194.

[32] A. H. Cowley, F. P. Gabbai, H. S. Isom, A. Decken, R. D. Culp, *Main Group Chem.* **1995**, *1*, 9 – 19.

[33] I. R. Butler, W. R. Cullen, J. Ni, S. J. Rettig, *Organometallics* **1985**, *4*, 2196 – 2201.

[34] a) J. G. Snijders, E. J. Baerends, P. Ros, *Mol. Phys.* **1979**, *38*, 1909 – 1929; b) T. Ziegler, V. Tschinke, E. J. Baerends, J. G. Snijders, W. Ravenek, *J. Phys. Chem.* **1989**, *93*, 3050 – 3056; c) E. van Lenthe, E. J. Baerends, J. G. Snijders, *J. Chem. Phys.* **1993**, *99*, 4597 – 4610.

[35] S. H. Vosko, L. Wilk, M. Nusair, *Can. J. Phys.* **1980**, *58*, 1200 – 1211.

[36] A. D. Becke, *Phys. Rev. A* **1988**, *38*, 3098 – 3100.

[37] J. P. Perdew, *Phys. Rev. B* **1986**, *33*, 8822 – 8824.

[38] L. J. Farrugia, *J. Appl. Crystallogr.* **1997**, *30*, 565.

[39] Mercury, 3.1.1 ed., http://www.ccdc.cam.ac.uk/mercury.

Received: October 7, 2013
Published online on January 24, 2014

 © 2014 Wiley-VCH Verlag GmbH & Co. KGaA, Weinheim